
This is an electronic reprint of the original article.
This reprint *may differ* from the original in pagination and typographic detail.

Author(s): Khriachtchev Leonid; Lundell, Jan; Tapio, Salla; Domanskaya, Alexandra V.; Räsänen, Markku; Isokoski, Karoliina

Title: HXeOBr in a xenon matrix

Year: 2011

Version:

Please cite the original version:

Khriachtchev, L., Lundell, J., Tapio, S., Domanskaya, A., Räsänen, M., & Isokoski, K. (2011). HXeOBr in a xenon matrix. *Journal of Chemical Physics*, 134 (12), 124307. doi:10.1063/1.3570826

All material supplied via JYX is protected by copyright and other intellectual property rights, and duplication or sale of all or part of any of the repository collections is not permitted, except that material may be duplicated by you for your research use or educational purposes in electronic or print form. You must obtain permission for any other use. Electronic or print copies may not be offered, whether for sale or otherwise to anyone who is not an authorised user.

HXeOBr in a xenon matrix

Leonid Khriachtchev,^{1,a)} Salla Tapio,¹ Alexandra V. Domanskaya,¹ Markku Räsänen,¹ Karoliina Isokoski,² and Jan Lundell³¹Department of Chemistry, University of Helsinki, P.O. Box 55, FIN-00014, Finland²Sackler Laboratory for Astrophysics, Leiden Observatory, Leiden University, P.O. Box 9513, 2300 RA Leiden, The Netherlands³Department of Chemistry, University of Jyväskylä, P.O. Box 35, FIN-40014 Jyväskylä, Finland

(Received 23 December 2010; accepted 7 March 2011; published online 28 March 2011)

We report on a new noble-gas molecule HXeOBr prepared in a low-temperature xenon matrix from the HBr and N₂O precursors by UV photolysis and thermal annealing. This molecule is assigned with the help of deuteration experiments and *ab initio* calculations including anharmonic methods. The H–Xe stretching frequency of HXeOBr is observed at 1634 cm^{−1}, which is larger by 56 cm^{−1} than the frequency of HXeOH identified previously. The experiments show a higher thermal stability of HXeOBr molecules in a xenon matrix compared to HXeOH. © 2011 American Institute of Physics. [doi:10.1063/1.3570826]

I. INTRODUCTION

Noble-gas hydrides with the general formula HNgY (Ng = Ar, Kr, or Xe; Y = an electronegative fragment) is a part of modern chemistry of noble gases.^{1–13} Twenty-five noble-gas hydrides are known including the argon compound HArF (Ref. 4) and the recent additions HXeOXeH,⁶ HKrCCF, and HXeCCF.⁷ A procedure to prepare these molecules consists of photodissociation of HY precursors and thermal mobilization of H atoms in a noble-gas matrix, which leads to the H + Ng + Y → HNgY reaction. The HNgY molecules are weakly bound and presumably exhibit a strong (HNg)⁺Y[−] charge-transfer character. They are metastable species with respect to the Ng + HY (two-body, 2B) asymptote and their decomposition is hindered by a relatively high bending barrier.¹ The H + Ng + Y (three-body, 3B) asymptote is higher in energy than HNgY in the experimentally studied cases.⁵ Intermolecular complexes involving HNgY molecules have been studied and show large blueshifts of the H–Xe stretching frequencies, featuring the strengthening of the H–Xe bond.^{8,9}

A group of noble-gas hydrides was prepared from the water precursor in a xenon matrix. The first identified species was HXeOH,¹⁰ followed by an open-shell species HXeO (Ref. 11) and a molecule with two Xe atoms, HXeOXeH.⁶ The decomposition of HXeOH upon annealing above 55 K in a xenon matrix is an interesting but unclear issue.¹² The theory predicts that HXeOH can be destabilized upon interaction with small water clusters,¹³ but it remains unknown whether this property is general for noble-gas hydrides or specific for HXeOH. The energetic stability of noble-gas compounds is of key importance for hypothetical perspectives to find noble-gas hydrides in practical environments.

Jayasekharan and Ghanty investigated a series of noble-gas hydrides HXeOX (X = F, Cl, or Br) at the MP2 level of theory and compared them to previously identified HXeOH.¹⁴ The 2B barrier for the HXeOX species was found to be

about 138 kJ mol^{−1}, which is about 20 kJ mol^{−1} smaller than that for HXeOH. The energetic gap to the 3B asymptote obtained for the HXeOX species is also smaller than that for HXeOH. Thus, no energetic stabilization was found for HXeOX as compared to HXeOH. On the other hand, the H–Xe stretching frequency for the HXeOX species was predicted to be somewhat higher than that of HXeOH, which features strengthening of the H–Xe bond.

In the present work, we revisit the study of computational properties of HXeOX (X = F, Cl, or Br), applying the CCSD(T) level of theory and the anharmonic method. In experiments, we attempt to prepare HXeOBr and HXeOCl. HXeOBr is reliably identified in a xenon matrix; however, we fail to find HXeOCl.

II. COMPUTATIONAL DETAILS AND RESULTS

The structural, energetic, and spectroscopic properties of the HXeOX (X = H, F, Cl, or Br) molecules were studied by *ab initio* methods utilizing the GAUSSIAN 03 Revision E.01 program package.¹⁵ The calculations were performed at the MP2/LJ18[Xe],6–311++G(2d,2p) and CCSD(T)/LJ18[Xe],6–311++G(2d,2p) levels of theory, which have previously been used to calculate the vibrational properties of noble-gas hydrides.^{3–10} For the optimized structures, we obtained all real harmonic vibrational frequencies indicating the true minimum on the potential energy surface. These studies were followed by anharmonic calculations to support the experimental assignments.^{3,6,16} The anharmonic calculations were done at the MP2 level of theory and then the MP2 anharmonicity of the H–Xe stretching mode was applied to the harmonic CCSD(T) frequency. This approach saves computational time because anharmonic calculations at the CCSD(T) level of theory are very time consuming. All calculations were performed on the computers at the CSC-Center for Scientific Computing Ltd (Espoo, Finland).

The computational results for HXeOX species (X = H, F, Cl, or Br) are presented in Tables I–IV. The geometries

^{a)} Author to whom correspondence should be addressed. Electronic mail: leonid.khriachtchev@helsinki.fi.

TABLE I. Computational results on HXeOH.

Vibrational properties	MP2/LJ18[Xe],6-311++G(2d,2p)		CCSD(T)/LJ18[Xe],6-311++G(2d,2p)
	Frequency (cm ⁻¹)	Intensity (km mol ⁻¹)	Frequency (cm ⁻¹)
	437.3	126.4	419.7
	584.5	10.0	575.5
	653.5	6.5	626.8
	818.4	8.7	820.5
	1820.1 [1718.5] ^a	1451.4	1673.1 [1579.5] ^b
	3843.3	50.7	3836.0
Geometry	$r_{\text{OH}} = 0.96 \text{ \AA}$, $r_{\text{XeO}} = 2.21 \text{ \AA}$, $r_{\text{XeH}} = 1.72 \text{ \AA}$, $\angle_{\text{XeOH}} = 109.4^\circ$		$r_{\text{OH}} = 0.96 \text{ \AA}$, $r_{\text{XeO}} = 2.21 \text{ \AA}$, $r_{\text{XeH}} = 1.72 \text{ \AA}$, $\angle_{\text{XeOH}} = 107.5^\circ$
Dissociation energy ^c	$-68.5 \text{ kJ mol}^{-1}$		$-54.7 \text{ kJ mol}^{-1}$

^aAnharmonic values in brackets.^bCombination of the CCSD(T) frequency and the MP2 anharmonicity.^c $\Delta E_{\text{MP2}} = (E_{\text{H}} + E_{\text{Xe}} + E_{\text{OH,opt}}) - E_{\text{HXeOH}}$.

TABLE II. Computational results on HXeOF.

Vibrational properties	MP2/LJ18[Xe],6-311++G(2d,2p)		CCSD(T)/LJ18[Xe],6-311++G(2d,2p)
	Frequency (cm ⁻¹)	Intensity (km mol ⁻¹)	Frequency (cm ⁻¹)
	173.5	3.3	168.7
	428.7	149.2	397.5
	647.1	4.8	607.3
	690.7	11.7	644.0
	969.5	17.3	832.2
	1916.7 [1810.6] ^a	1277.0	1757.6 [1659.0] ^b
Geometry	$r_{\text{OF}} = 1.45 \text{ \AA}$, $r_{\text{XeO}} = 2.24 \text{ \AA}$, $r_{\text{XeH}} = 1.69 \text{ \AA}$, $\angle_{\text{XeOF}} = 100.7^\circ$		$r_{\text{OF}} = 1.48 \text{ \AA}$, $r_{\text{XeO}} = 2.27 \text{ \AA}$, $r_{\text{XeH}} = 1.71 \text{ \AA}$, $\angle_{\text{XeOF}} = 98.3^\circ$
Dissociation energy ^c	$-39.2 \text{ kJ mol}^{-1}$		$-33.2 \text{ kJ mol}^{-1}$

^aAnharmonic values in brackets.^bCombination of the CCSD(T) frequency and the MP2 anharmonicity.^c $\Delta E_{\text{MP2}} = (E_{\text{H}} + E_{\text{Xe}} + E_{\text{OF,opt}}) - E_{\text{HXeOF}}$.

TABLE III. Computational results on HXeOCl.

Vibrational properties	MP2/LJ18[Xe],6-311++G(2d,2p)		CCSD(T)/LJ18[Xe],6-311++G(2d,2p)
	Frequency (cm ⁻¹)	Intensity (km mol ⁻¹)	Frequency (cm ⁻¹)
	143.6	4.4	141.2
	410.8	121.4	376.0
	629.0	4.3	596.6
	665.0	15.2	630.2
	770.5	68.0	691.0
	1905.7 [1795.1] ^a	1483.3	1760.7 [1658.5] ^b
Geometry	$r_{\text{OCl}} = 1.70 \text{ \AA}$, $r_{\text{XeO}} = 2.24 \text{ \AA}$, $r_{\text{XeH}} = 1.6893 \text{ \AA}$, $\angle_{\text{XeOCl}} = 152.3^\circ$		$r_{\text{OCl}} = 1.72 \text{ \AA}$, $r_{\text{XeO}} = 2.27 \text{ \AA}$, $r_{\text{XeH}} = 1.71 \text{ \AA}$, $\angle_{\text{XeOCl}} = 108.8^\circ$
Dissociation energy ^c	$-49.0 \text{ kJ mol}^{-1}$		$-19.9 \text{ kJ mol}^{-1}$

^aAnharmonic values in brackets.^bCombination of the CCSD(T) frequency and the MP2 anharmonicity.^c $\Delta E_{\text{MP2}} = (E_{\text{H}} + E_{\text{Xe}} + E_{\text{OCl,opt}}) - E_{\text{HXeOCl}}$.

TABLE IV. Computational results on HXeOBr.

	MP2/LJ18[Xe],6-311++G(2d,2p)		CCSD(T)/LJ18[Xe],6-311++G(2d,2p)
Vibrational properties	Frequency (cm ⁻¹)	Intensity (km mol ⁻¹)	Frequency (cm ⁻¹)
	108.3	3.5	106.4
	398.6	98.0	360.7
	627.9	4.1	596.5
	642.1	72.9	600.4
	702.2	79.6	646.8
	1895.8 [1783.8] ^a	1564.8	1764.1 [1659.9] ^b
Geometry	$r_{\text{OBr}} = 1.82 \text{ \AA}$, $r_{\text{XeO}} = 2.23 \text{ \AA}$ $r_{\text{XeH}} = 1.69 \text{ \AA}$, $\angle_{\text{XeOBr}} = 152.3^\circ$		$r_{\text{OBr}} = 1.84 \text{ \AA}$, $r_{\text{XeO}} = 2.27 \text{ \AA}$, $r_{\text{XeH}} = 1.71 \text{ \AA}$, $\angle_{\text{XeOBr}} = 110.8^\circ$
Dissociation energy ^c	-63.9 kJ mol ⁻¹		-26.1 kJ mol ⁻¹

^aAnharmonic values in brackets.^bCombination of the CCSD(T) frequency and the MP2 anharmonicity.^c $\Delta E_{\text{MP2}} = (E_{\text{H}} + E_{\text{Xe}} + E_{\text{OBr,opt}}) - E_{\text{HXeOBr}}$.

and H–Xe stretching frequencies calculated here at the MP2 level of theory match the results reported by Jayasekharan and Ghanty.¹⁴ The CCSD(T) geometries differ noticeably from the MP2 results, especially with respect to the XeOX angles. The energetic correction provided by the CCSD(T) method is also remarkable. For all molecules studied here, the difference with the 3B asymptote is smaller at the CCSD(T) level of theory. This decrease is not significant for HXeOH (from 68.5 to 54.7 kJ mol⁻¹) and HXeOF (from 39.2 to 33.2 kJ mol⁻¹). For HXeOCl and HXeOBr, the CCSD(T) correction is much larger: from 49.0 to 19.9 kJ mol⁻¹ for HXeOCl and from 63.9 to 26.1 kJ mol⁻¹ for HXeOBr. It is seen that the CCSD(T) method gives very different relative energetics of the HXeOX molecules than the MP2 level of theory. As discussed by Lignell *et al.*,⁵ the MP2 method tends to overestimate the energy of open-shell species, which leads to an incorrect position of the 3B asymptote and hence overestimates the energetic stability of noble-gas hydrides.

The harmonic MP2 method also overestimates the H–Xe stretching frequencies because of (i) insufficient level of theory and (ii) neglected anharmonicity. For example, the MP2 frequency is 1895.1 cm⁻¹ for HXeOH, whereas the experimental value is 1578 cm⁻¹. The CCSD(T) calculations yield frequencies more than 100 cm⁻¹ lower, and a similar downshift occurs when taking anharmonicity into account at the MP2 level of theory. The combination of the harmonic CCSD(T) and anharmonic (MP2) methods yields 1579.5 cm⁻¹ for the H–Xe stretching frequency of HXeOH, which is very close to the experimental value (1578 cm⁻¹). A similarly good result was obtained by using this approach, for example, for HXeOXeH.⁶ The anharmonic estimates for the H–Xe stretching frequencies of HXeOX (X = F, Cl, or Br) are given in Tables II–IV.

III. EXPERIMENTAL DETAILS AND RESULTS

Gaseous mixtures with different amounts of HBr (or HCl), N₂O, and H₂O in xenon were deposited onto a cold CsI substrate typically at 30 K in a closed-cycle helium cryostat (APD, DE 202A). The relative concentrations of the embedded molecules in xenon were typically ~1:1000. Krypton ma-

trices containing HBr and N₂O were also studied. The IR absorption spectra in the 4000 to 400 cm⁻¹ range were measured with a Nicolet SX60 FTIR spectrometer (resolution 1 cm⁻¹). In most of the experiments, the matrices were irradiated with a 193-nm excimer laser (MPB, model MSX-250, pulse energy density ~10 mJ cm⁻²) at 8.5 K using typically 1500 pulses. In some experiments, photolysis was done with vacuum ultraviolet light from a high-pressure xenon lamp (Ophos).⁶ The photolyzed matrices were annealed at 35 to 75 K (for about 5 min), and the IR spectra were measured at 8.5 K.

The HBr/Xe matrices with low HBr concentrations (~1/1000) deposited at 30 K contain predominantly monomeric HBr. Monomeric HBr in a xenon matrix absorbs at 2531.1 [the strongest absorption, $R(0)$], 2520.0, and 2508.9 cm⁻¹ (Fig. 1), and the absorptions of HBr dimers and trimers are at 2493.0 and 2475.1 cm⁻¹, respectively.¹⁷ The strongest bands of N₂O are at 1280 (NO stretch) and 2215 (NN stretch) cm⁻¹. The band at 2553 cm⁻¹ seen in Fig. 1 is the NO stretching overtone. For HBr/N₂O/Xe matrices, the weak bands at 2523 and 2543 cm⁻¹ can be attributed to HBr ··· N₂O complexes (Fig. 1).

The HBr bands are efficiently bleached by 193-nm light reflecting the HBr photodissociation and H atom escape from the parent cage, which stabilizes H and Br atoms in a xenon matrix.¹⁸ Photolysis of N₂O produces isolated N₂ and O.^{6,19,20} The efficiency of the HY and N₂O decomposition decreases for thicker matrices and higher concentrations due to self-limitation of photolysis,²¹ which practically limits the matrix thickness at the level of ~100 μm. Small traces of HXeBr are seen after 193 nm photolysis of HBr in a xenon matrix. This photolysis-induced formation has been observed for some noble-gas hydrides and occurs due to the locality of solid-state photodissociation.^{4,22,23}

Annealing of photolyzed HBr/Xe matrices at ~40 K mobilizes H atoms,^{24,25} and HXeBr molecules are formed (Fig. 2), presumably via the reaction of the neutral atoms.^{26,27} HXeBr has the strongest absorption at 1504 cm⁻¹, which corresponds to the H–Xe stretching mode.²⁸ The satellite at 1520 cm⁻¹ (marked with L in Fig. 2) originates from the librational motion of monomeric HXeBr in a xenon matrix.²⁹ For matrices with small HBr/Xe ratios (~1/1000), the HXeY

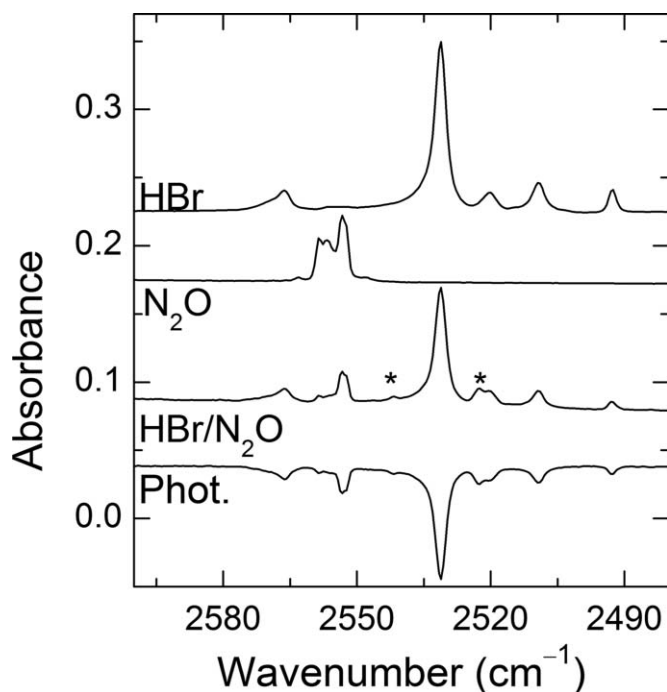


FIG. 1. FTIR spectra (from top to bottom) of HBr/Xe, N₂O/Xe, and HBr/N₂O/Xe matrices after deposition and the result of 193 nm photolysis for the HBr/N₂O/Xe matrix. The tentative bands of the HBr ··· N₂O complex are marked with asterisks. The spectra were measured at 8.5 K.

monomer absorption strongly dominates in the spectrum after annealing of the photolyzed matrix; however, additional H–Xe stretching absorptions that have been previously assigned to the HXeBr ··· HBr complexes are also observed (marked with C in Fig. 2).¹⁷ HXeH molecule is another noble-gas hydride efficiently formed in these experiments (bands at 1166 and 1181 cm^{−1}).³⁰

For photolyzed HBr/N₂O/Xe matrices, annealing at ~40 K also promotes the formation of HXeBr and HXeH (middle trace in Fig. 2). Due to the presence of N₂ molecules from the N₂O photolysis, minor amounts of HXeBr ··· N₂ complexes are observed (1515.5 cm^{−1}).³¹ Mobilization of H atoms also leads to the formation of the *cis* and *trans* conformers of HN₂O,^{6,32} whose NN stretching bands are marked by dots in Fig. 2. The presence of O atoms produces additional noble-gas hydrides such as HXeO and HXeOXeH with the H–Xe stretching absorptions at 1466 and 1380 cm^{−1}, respectively.^{6,11} It should be reminded that O atoms become mobile in solid xenon at 30–35 K.^{6,11,20} This stage of annealing is shown by the lowest trace in Fig. 2. In particular, this mobilization promotes the reactions of O atoms with neutral H–Xe centers and leads to the formation of HXeO radicals that are the precursors for HXeOXeH.⁶ Some formation of HOO radicals (1383.1 and 1095.8 cm^{−1}) and ozone (1027 cm^{−1}) are also observed upon mobilization of O atoms.

One previously unknown band at 1634 cm^{−1} persistently appears upon annealing at 40–45 K of photolyzed HBr/N₂O/Xe matrices. This band is not observed after annealing of photolyzed HBr/Xe (Fig. 2), N₂O/Xe, H₂O/Xe, H₂O/N₂O/Xe (Fig. 3), or HCl/N₂O/Xe (Fig. 4) matrices. No corresponding band is produced by photolysis and annealing of HBr/N₂O/Kr matrices, which suggests participation of

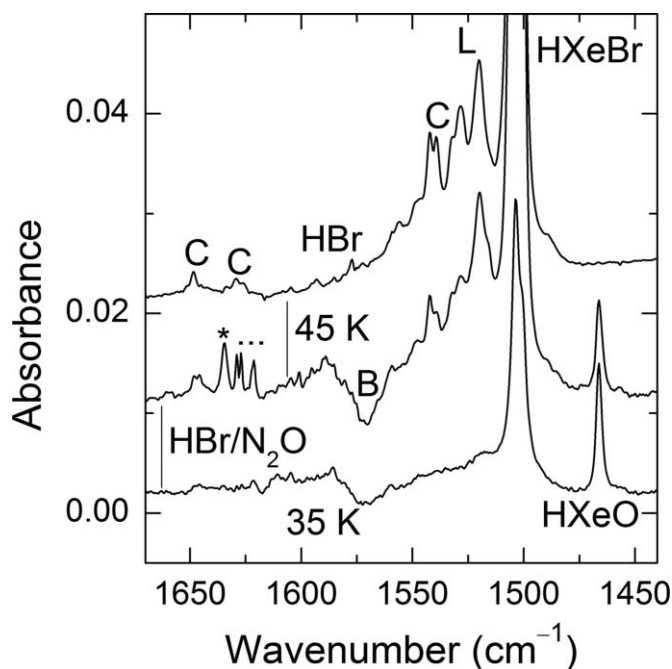


FIG. 2. FTIR spectra showing the result of annealing of photolyzed HBr/Xe (the upper spectrum) and HBr/N₂O/Xe (two lower spectra) matrices. The annealing temperatures are 45 K (two upper spectra) and 35 K (the lowest spectrum). The band assigned to HXeOBr is marked with asterisk and the bands of HN₂O with dots. The HXeBr ··· HBr complex bands (Ref. 17) and the HXeBr libration band (Ref. 29) are marked with C and L, respectively. The broad feature marked with B originates from the substrate absorption. The spectra were measured at 8.5 K.

Xe in this species. The absorber in question is easily decomposed by UV light (for example, from a mercury lamp). Upon deuteration of HBr precursor, the corresponding band is observed at 1190 cm^{−1}, giving the H/D frequency ratio of 1.373. These facts show that this absorber needs H, Xe, O, and Br atoms for the formation and it is assigned in the present work to HXeOBr.

We compared the thermal stabilities of HXeOH and HXeOBr. For this purpose, a H₂O/N₂O/HBr/Xe matrix was photolyzed and annealed at 45 K, which produces the bands of both HXeOH and HXeOBr (middle spectrum in Fig. 3). Upon annealing at 55 K, HXeOH decomposes within minutes as reported previously,¹² whereas HXeOBr remains practically stable (the lowest spectrum in Fig. 3). HXeOBr is quite stable upon annealing at 60 K; however, its absorption substantially decreases upon annealing at 75 K.

Experiments with HCl/N₂O/Xe matrices were performed in order to prepare HXeOCl. After deposition, the strongest absorption of HCl monomer is the *R*(0) transition at 2858 cm^{−1} for H³⁵Cl, and the H³⁷Cl absorption is ~2 cm^{−1} lower in energy. The band at 2837 cm^{−1} is tentatively assigned to the HCl ··· N₂O complex. For high deposition temperatures and HCl concentrations, the bands of HCl dimers at 2816.5 cm^{−1} and trimers at 2792.4 cm^{−1} grow.¹⁷ After photolysis and annealing of these matrices, the noble-gas hydrides HXeCl (1648 cm^{−1}),²⁸ HXeH, HXeO, and HXeOXeH are seen in the spectra as well as HN₂O, O₃, etc. (Fig. 4). However, no bands that could be assigned to HXeOCl were found as discussed below.

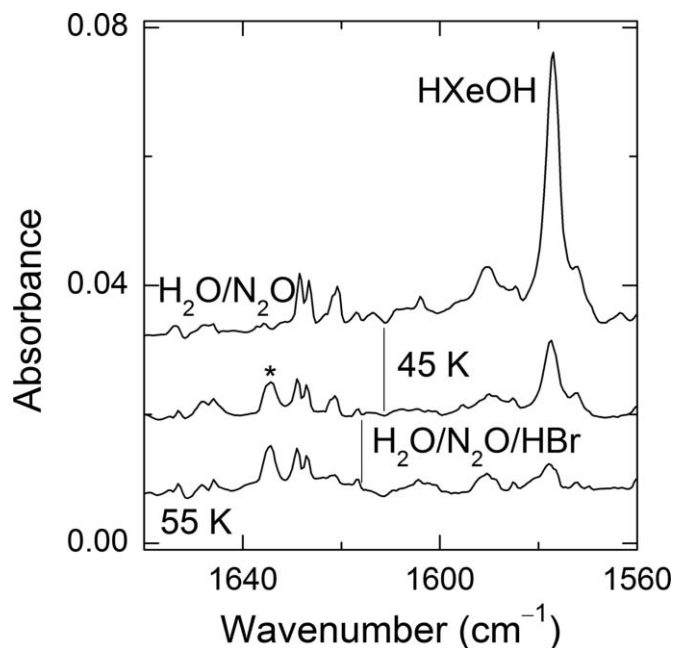


FIG. 3. FTIR spectra showing the result of annealing of photolyzed $\text{H}_2\text{O}/\text{N}_2\text{O}/\text{Xe}$ (the upper spectrum) and $\text{H}_2\text{O}/\text{N}_2\text{O}/\text{HBr}/\text{Xe}$ (two lower spectra) matrices. The annealing temperatures are 45 K (two upper spectra) and 55 K (the lowest spectrum). The band assigned to HXeOBr is marked with asterisk. The spectra were measured at 8.5 K.

IV. CONCLUDING DISCUSSION

Our assignment of the 1634 cm^{-1} band to the $\text{H}-\text{Xe}$ stretching mode of HXeOBr is based on the following arguments. Similar to other noble-gas hydrides HXeY , this absorber is synthesized by photolysis of proper precursors in a noble-gas matrix followed by annealing, which mobilizes the photolysis products. The presence of H, O, and Br atoms in a xenon matrix is required for the formation of the 1634 cm^{-1} band. Similar to other HNgY molecules, this absorber is easily decomposed by UV light. The H/D frequency ratio of the $\text{H}-\text{Xe}$ stretching mode is 1.373, which is very close to the experimental values known for other HNgY molecules. No corresponding band (with appropriate matrix shift) is observed in similar experiments in krypton matrices despite the formation of other species such as HN_2O and ozone. Theory strongly supports the experimental frequency for HXeOBr and confirms its energetic stability. The anharmonic value of 1660 cm^{-1} (Table IV) is in good agreement with the experiment. In both experiment and theory, the $\text{H}-\text{Xe}$ stretching frequency of HXeOBr is consistently higher than that of HXeOH . The $\text{H}-\text{Xe}$ stretching mode is only observed in experiments because it is much more intense than the other modes (Table IV), which is characteristic for noble-gas hydrides.¹ The 1634 cm^{-1} band does not coincide with the water absorptions in this region.¹² We have no other candidates for the 1634 cm^{-1} band than HXeOBr .

The electronegative fragment required for the formation of HXeOBr is the BrO radical. BrO is not produced directly by photolysis of a precursor, in contrast to most of the previous works on noble-gas hydrides. As the closest example, HXeOXeH forms from the HXeO precursor also supplied from two different precursors, HBr and N_2O .^{6,11} We do not

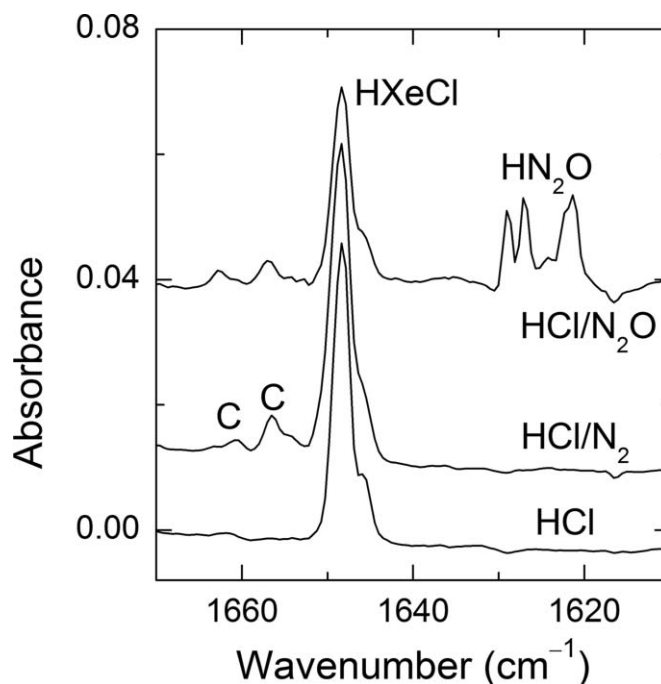


FIG. 4. FTIR spectra showing the result of annealing at 45 K (from top to bottom) of photolyzed $\text{HCl}/\text{N}_2\text{O}/\text{Xe}$, $\text{HCl}/\text{N}_2/\text{Xe}$, and HCl/Xe matrices. The bands of the $\text{HXeCl} \cdots \text{N}_2$ complex are marked with C (see Ref. 31 for details). The spectra were measured at 8.5 K.

observe the BrO band, which should be at $\sim 730\text{ cm}^{-1}$, most probably due to its low absorption intensity ($\sim 1\text{ km mol}^{-1}$).³³ Many possibilities exist for the formation of BrO radical in matrices containing bromine and oxygen species.³⁴ We are not aware of the probability of the direct $\text{Br} + \text{O}$ reaction; however, it may be favorable in solid xenon. Solid-phase reactions are often different from the gas-phase cases. In particular, HOBr is formed in our experiments as evidenced by the band at 1158 cm^{-1} ,³⁵ and this probably occurs via the $\text{O} + \text{HBr}$ reaction^{36,37} followed by the in-cage $\text{Br} + \text{OH}$ reaction.

HXeOBr is more stable upon annealing of the matrix than HXeOH (Fig. 3). This observation has no reasonable explanation based on the available theoretical results. It is plausible to assume that the kinetic stability of these molecules is controlled by the 3B channel.¹ Tsivion and Gerber calculated this barrier for HXeOH and obtained 0.59 eV (54 kJ mol^{-1}).³⁸ This value is close to our result on the HXeOH dissociation energy at the CCSD(T) level of theory, even though Tsivion and Gerber obtained a twice smaller dissociation energy. This 3B barrier is high enough to prevent decomposition at cryogenic temperatures. The transition state theory gives for HXeOH the lifetime of 10^5 h at 140 K.³⁸ The dissociation energy of HXeOBr at the CCSD(T) level of theory is about twice smaller than that of HXeOH , which seemingly features a lower stability. However, the experiment shows the opposite trend. HXeOBr can be additionally stabilized by the $\text{H} + \text{Xe} + \text{OBr}$ formation barrier, but this barrier cannot be substantial because HXeOBr is formed at low temperatures. HXeOXeH is also quite stable at 55 K although its theoretical 3B barrier is substantially smaller than that of HXeOH .³⁸ It is possible that HXeOH is destabilized by the solid xenon

surrounding as it has been theoretically shown for HXeOH in small water clusters.¹³ Further studies are required to understand the matrix-induced stabilization and destabilization effects on noble-gas hydrides. Accurate energy profiles for the noble-gas hydrides are still a challenge, where electron correlation and multireference nature play an important role especially in the case of many-body dissociation barriers. Recent developments such as the spin-component-scaled MP2 approach could be useful for evaluating the energy differences including open-shell species.^{39,40}

As mentioned previously, we did not identify HXeOCl in the current experiments (Fig. 4). We believe that this species is energetically stable and the reason of the failure is different. For example, the photodecomposition of HCl is less efficient in a xenon matrix compared to HBr and a longer photolysis is required, which may lead to losses of H atoms due to the light-induced mobility. As a result, the noble-gas hydrides are formed in the experiments with HCl less efficiently than in the experiments with HBr. No evidence of ClO was observed after annealing but this radical should have very small absorption. The band at 1657 cm^{-1} seen in Fig. 4 practically coincides with the $\text{HXeCl} \cdots \text{N}_2$ complex band,³¹ nitrogen being produced by photolysis of N_2O . The band at 1663 cm^{-1} is somewhat shifted from the weaker $\text{HXeCl} \cdots \text{N}_2$ complex band at 1661 cm^{-1} , which may feature the formation of HXeOCl. The calculations predict the H–Xe stretching mode of HXeOCl almost at the same frequency as that of HXeOBr, whereas the experimental frequencies would differ by $\sim 30\text{ cm}^{-1}$, which is an acceptable deviation. Nevertheless, we have no strong grounds to assign the band at 1663 cm^{-1} as well as other weak bands to HXeOCl. As an additional uncertainty, the $\text{HXeCl} \cdots \text{N}_2\text{O}$ complex can absorb in this spectral region. Experiments with other precursors may help answer this question; however, this exceeds the scope of the present work.

ACKNOWLEDGMENTS

The work was supported by the Finnish Center of Excellence in Computational Molecular Science. A.V.D. acknowledges a postdoctoral grant from the University of Helsinki. CSC-Center for Scientific Computing Ltd (Espoo, Finland) is thanked for computer resources. Juho Kajava is thanked for technical assistance.

¹L. Khriachtchev, M. Räsänen, and R. B. Gerber, *Acc. Chem. Res.* **42**, 183 (2009).

²W. Grochala, *Chem. Soc. Rev.* **36**, 1632 (2007).

³J. Lundell, L. Khriachtchev, M. Pettersson, and M. Räsänen, *Low Temp. Phys.* **26**, 680 (2000).

- ⁴L. Khriachtchev, M. Pettersson, N. Runeberg, J. Lundell, and M. Räsänen, *Nature (London)* **406**, 874 (2000).
- ⁵A. Lignell, L. Khriachtchev, J. Lundell, H. Tanskanen, and M. Räsänen, *J. Chem. Phys.* **125**, 184514 (2006).
- ⁶L. Khriachtchev, K. Isokoski, A. Cohen, M. Räsänen, and R. B. Gerber, *J. Am. Chem. Soc.* **130**, 6114 (2008).
- ⁷L. Khriachtchev, A. Domanskaya, J. Lundell, A. Akimov, M. Räsänen, and E. Misochko, *J. Phys. Chem. A* **114**, 4181 (2010).
- ⁸S. A. C. McDowell, *Curr. Org. Chem.* **10**, 791 (2006).
- ⁹A. Lignell and L. Khriachtchev, *J. Mol. Struct.* **889**, 1 (2008).
- ¹⁰M. Pettersson, L. Khriachtchev, J. Lundell, and M. Räsänen, *J. Am. Chem. Soc.* **121**, 11904 (1999).
- ¹¹L. Khriachtchev, M. Pettersson, J. Lundell, H. Tanskanen, T. Kiviniemi, N. Runeberg, and M. Räsänen, *J. Am. Chem. Soc.* **125**, 1454 (2003).
- ¹²L. Khriachtchev, H. Tanskanen, M. Pettersson, M. Räsänen, J. Ahokas, H. Kunttu, and V. Feldman, *J. Chem. Phys.* **116**, 5649 (2002).
- ¹³A. V. Nemukhin, B. L. Grigorenko, L. Khriachtchev, H. Tanskanen, M. Pettersson, and M. Räsänen, *J. Am. Chem. Soc.* **124**, 10706 (2002).
- ¹⁴T. Jayasekharan and T. K. Ghanty, *J. Chem. Phys.* **124**, 164309 (2006).
- ¹⁵M. J. Frisch, G. W. Trucks, H. B. Schlegel *et al.* GAUSSIAN 03, Revision C.02, Gaussian, Inc., Wallingford, CT, 2004.
- ¹⁶J. Lundell, M. Pettersson, L. Khriachtchev, M. Räsänen, G. M. Chaban, and R. B. Gerber, *Chem. Phys. Lett.* **322**, 389 (2000).
- ¹⁷A. Lignell, J. Lundell, L. Khriachtchev, and M. Räsänen, *J. Phys. Chem. A* **112**, 5486 (2008).
- ¹⁸V. A. Apkarian and N. Schwentner, *Chem. Rev.* **99**, 1481 (1999).
- ¹⁹A. V. Danilychev and V. A. Apkarian, *J. Chem. Phys.* **99**, 8617 (1993).
- ²⁰T. Kiviniemi, M. Pettersson, L. Khriachtchev, M. Räsänen, and N. Runeberg, *J. Chem. Phys.* **121**, 1839 (2004).
- ²¹L. Khriachtchev, M. Pettersson, and M. Räsänen, *Chem. Phys. Lett.* **288**, 727 (1998).
- ²²L. Khriachtchev, M. Pettersson, J. Lundell, and M. Räsänen, *J. Chem. Phys.* **114**, 7727 (2001).
- ²³M. Pettersson, L. Khriachtchev, J. Lundell, S. Jolkkonen, and M. Räsänen, *J. Phys. Chem. A* **104**, 3579 (2000).
- ²⁴J. Eberlein and M. Creuzburg, *J. Chem. Phys.* **106**, 2188 (1997).
- ²⁵L. Khriachtchev, H. Tanskanen, M. Pettersson, M. Räsänen, V. Feldman, F. Sukhov, A. Orlov, and A. F. Shestakov, *J. Chem. Phys.* **116**, 5708 (2002).
- ²⁶M. Pettersson, J. Nieminen, L. Khriachtchev, and M. Räsänen, *J. Chem. Phys.* **107**, 8423 (1997).
- ²⁷L. Khriachtchev, H. Tanskanen, and M. Räsänen, *J. Chem. Phys.* **124**, 181101 (2006).
- ²⁸M. Pettersson, J. Lundell, and M. Räsänen, *J. Chem. Phys.* **102**, 6423 (1995).
- ²⁹L. Khriachtchev, A. Lignell, J. Juselius, M. Räsänen, and E. Savchenko, *J. Chem. Phys.* **122**, 014510 (2005).
- ³⁰M. Pettersson, J. Lundell, and M. Räsänen, *J. Chem. Phys.* **103**, 205 (1995).
- ³¹L. Khriachtchev, S. Tapio, M. Räsänen, A. Domanskaya, and J. Lundell, *J. Chem. Phys.* **133**, 084309 (2010).
- ³²S. L. Laursen, A. E. Delia, and K. Mitchell, *J. Phys. Chem. A* **104**, 3681 (2000).
- ³³O. Galvez, A. Zoerner, A. Loewenschuss, and H. Grothe, *J. Phys. Chem. A* **110**, 6472 (2006).
- ³⁴R. P. Wayne, G. Poulet, P. Biggs, J. P. Burrows, R. A. Cox, P. J. Crutzen, G. D. Hayman, M. E. Jenkin, G. Le Bras, G. K. Moortgat, U. Platt, and R. N. Schindler, *Atmos. Environ.* **29**, 2677 (1995).
- ³⁵I. Schwager and A. Arkell, *J. Am. Chem. Soc.* **89**, 6006 (1967).
- ³⁶D. F. Nava, R. S. Bosco, and L. J. Stief, *J. Chem. Phys.* **78**, 2443 (1983).
- ³⁷A. F. Jalbout, *J. Mol. Struct.: THEOCHEM* **571**, 103 (2001).
- ³⁸E. Tsivion and R. B. Gerber, *Chem. Phys. Lett.* **482**, 30 (2009).
- ³⁹S. Grimme, *J. Chem. Phys.* **118**, 9095 (2003).
- ⁴⁰R. A. DiStasio Jr. and M. Head-Gordon, *Mol. Phys.* **105**, 1073 (2007).